The Fabrication and Bandgap Engineering of Photonic Multilayers**

By *Peng Jiang, Gordana N. Ostojic, Roxana Narat, Daniel M. Mittleman,* and *Vicki L. Colvin**

This communication describes a method to fabricate multilayer colloidal crystals formed by the layer-by-layer deposition of silica beads on a glass substrate. Each layer of the crystal consists of a three-dimensionally ordered array of close-packed colloids. These multilayer samples are amenable to templating methods for tuning the dielectric contrast of the material. The resulting photonic crystal structures exhibit optical properties which resemble the superposition of the properties of each individual crystal, with additional structure that suggests the onset of superlattice-type miniband formation. These multilayer structures thus afford new opportunities for engineered photonic behavior.

Traditionally colloidal crystals are three dimensional periodic structures formed from monodisperse colloids.[1–3] Because of their diffractive optical properties they are a type of photonic crystal[4–6] and may have applications as optical filters and switches,[7–9] high density magnetic data storage devices,[10] chemical and biochemical sensors,[11,12] or as removable scaffolds for the formation of highly ordered, macroporous materials.[13–22] They are also useful as model systems for fundamental studies of crystal melting and phase transition behavior.[23–26] The process of colloidal crystallization has been extensively studied, leading to the development of several methods to make high quality colloidal crystals with few crystalline defects. These techniques include electrostatically induced crystallization,[8,27–30] gravity sedimentation,[24,31] electro-hydrodynamic deposition,[32,33] colloidal epitaxy,[34] physical confinement[3,35] and convective self-assembly.[36,37] Bimodal AB_2 and AB_{13} colloidal crystals with complex structures have also been observed in binary mixtures of hard-sphere colloids with specific radii ratios.[38–40] Here we report a method to make a new form of colloidal crystal, a multilayer crystal, using successive deposition of crystals of colloids of arbitrary sizes.

The multilayer colloidal crystal is schematically represented in Figure 1A. Spheres of different colors represent submicrometer silica or polystyrene colloids of different sizes. Each layer of the crystal is a close-packed array of colloids, and the overall structure consists of successively stacked crystals, formed of colloids of arbitrary diameters. The preparation of these structures is described in the experimental section.

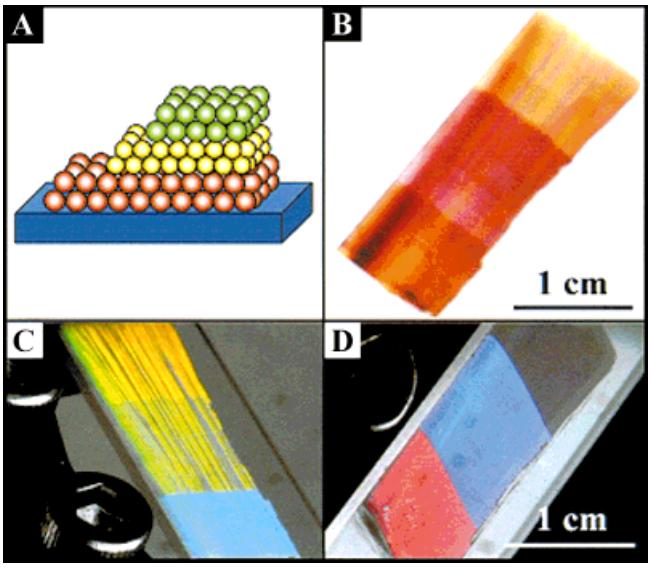

Fig. 1. A) A schematic representation of a multilayer colloidal crystal made by consecutive deposition of colloidal crystals from colloids of three different sizes. Photographs showing the colors transmitted (B) and reflected (C and D from different angles) from a 430 nm/253 nm/338 nm silica superlattice crystal. The top part of the sample is the region where only the bottom crystalline layer is present (colloidal crystal of 430 nm spheres), the middle part shows the doubly coated area (430 nm/253 nm) and the bottom part shows the triply coated area.

The high uniformity of the resulting crystals can be illustrated by the transmission (Fig. 1B) and reflection (Fig. 1C and D from different angles) photographs of a three-layer crystal. This sample is formed by consecutive deposition of 13 layers of 430 nm silica spheres, followed by 16 layers of 253 nm silica spheres, followed by 10 layers of 338 nm silica spheres. We describe the multilayer colloidal crystal pattern by listing the sphere size from bottom to top. For example, the sample in Figure 1 is referred to as 430 nm/253 nm/338 nm. The reflected colors are caused by Bragg diffraction of visible light by the three-dimensionally ordered arrays of submicrometer colloids. When two overlapping layers are made from colloids with extremely different sizes, most of the reflected light from the bottom layer will transmit through the upper layer, resulting in the transparent appearance of the second layer in Figure 1C (430 nm/253 nm).

Crystalline quality is among the most important parameters in determining the performance of colloidal crystals in optical applications. Figure 2 shows the typical top-view and cross-sectional scanning electron microscopy (SEM) images of each "step" of the sample shown in Figure 1. In Figure 2A, the hexagonal close-packed (hcp) arrangement of the top 430 nm layer is evident. The sharp peaks in the two-dimensional fast Fourier transform (FFT, inset) of a low-magnification image confirm the presence of long-range crystalline order extending over the largest length scales ($40 \times 40\ \mu m^2$) accessible in a single image. The stacking of close-packed layers shown in Figure 2B demonstrates the high degree of order along the (111) crystallographic axis, perpendicular to the substrate.

[*] Dr. V. L. Colvin, Dr. P. Jiang, R. Narat
Department of Chemistry
Center for Nanoscale Science and Technology
Rice University
Houston, TX 77005 (USA)
E-mail: colvin@rice.edu
G. N. Ostojic, Dr. D. M. Mittleman
Department of Electrical and Computer Engineering
Rice University
Houston, TX 77005 (USA)

[**] The authors acknowledge funding from the NSF (CHE-9702520) and the Welch Foundation (C-1342).

  0935-9648/01/0603-0389 $ 17.50+.50/0

ADVANCED MATERIALS

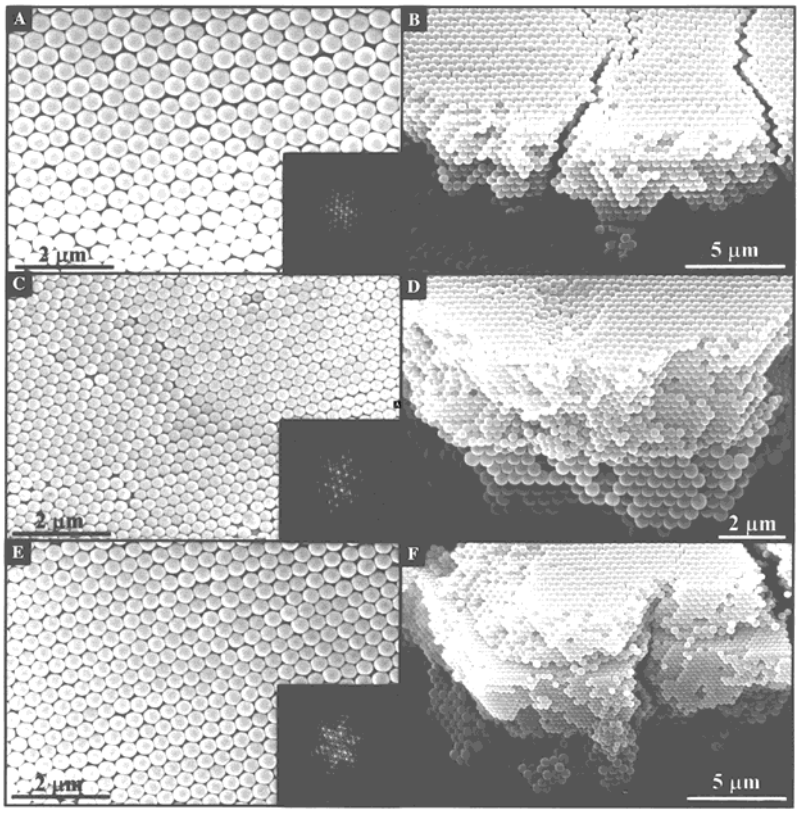

Fig. 2. Typical SEM images showing top and side views of each layer of a 430 nm/253 nm/338 nm crystal. A) and B) show the single coated area (430 nm silica multilayers); C) and D) show the doubly coated area (430 nm/253 nm); E) and F) show the triply coated area. The insets of A), C), and E) show fast FFTs of 40 × 40 μm^2 regions.

The long-range order of the second and the third "steps" of this stacked crystal is confirmed by the top-view SEM images and FFTs shown in Figure 2C and E. This ordering extends over the whole area of each multilayer, as demonstrated by the uniform visual appearance of the samples (see Fig. 1). Figure 2D and F clearly show the overlapping of close-packed multilayers with different sphere sizes. Each layer is highly ordered and remains oriented with its (111) axis parallel to the slide.

Though images such as these confirm a regular close-packed arrangement, it is difficult to distinguish between the face-centered cubic (fcc) (ABCABC...) and hcp (ABABAB...) structures even for each individual multilayer. Theoretical calculations, though, have indicated that the fcc structure is stabilized slightly.[41] Also, it is important to note that these crystals are not perfect; defects such as cracks and point defects are observed. However, there are apparently no grain boundaries over areas as large as 1 cm^2, and the (111) axis is oriented perpendicularly to the underlying substrate.[36]

An important feature of the convective assembly process is that it permits control over the thickness of the resulting crystals. The number of colloid layers deposited, k, is related to the particle volume fraction and sphere size, according to Equation 1:[36,42]

$$k = \frac{\beta L \varphi}{0.605\, d\, (1-\varphi)} \qquad (1)$$

where L is the meniscus height, β is the ratio between the velocity of a particle in solution and the fluid velocity and is taken to be 1, d is the particle diameter, and φ is the particle volume fraction in solution. This precise control is one factor which permits the photonic bandgap behavior to be tuned in the multilayered crystals.[43]

Since the multilayer colloidal crystals are stacks of colloidal crystals with different particle sizes, the interfacial packing is an important characteristic of these samples. There are essentially two types of stacking: big spheres on smaller ones and small spheres on bigger ones. We have tested a large number of combinations using colloids from 200 nm to 500 nm and found that there is no significant difference in the visual appearance or transmission spectra of the resulting multilayer crystals. Figure 3 shows SEM images of two stages in the crystallization process of big silica spheres (338 nm) on a crystal of smaller spheres (253 nm). An hcp monolayer is formed at the immediate crystalline growth front (Fig. 3A), while a three monolayer crystal is formed at 20 μm from the growth front (Fig. 3B). Further SEM observation shows the thickness is uniform starting at about 100 μm from the growth front (Fig. 2F). This gradient film thickness has been observed in our previous work, and can be explained by

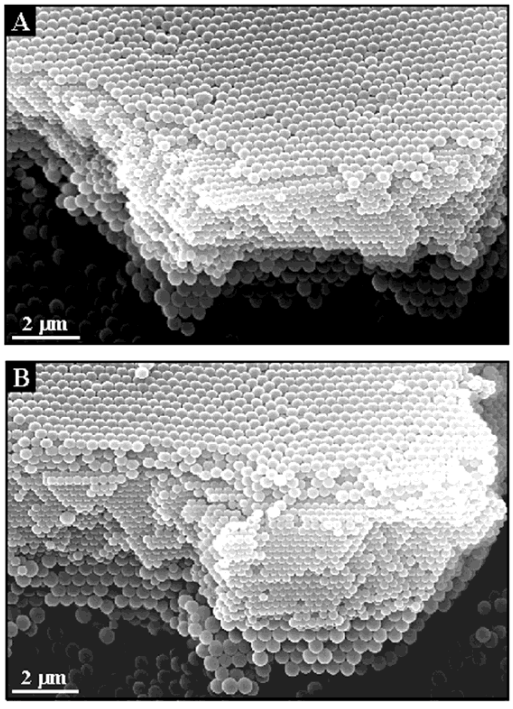

Fig. 3. Typical SEM images showing the interfacial stacking of 338 nm colloids on a crystal of 253 nm spheres. A) Monolayer packing at the immediate crystal growth front. B) Three monolayers, at a location approximately 20 μm from the crystal growth front.

  0935-9648/01/0603-0390 $ 17.50+.50/0

the thinning of the meniscus at the immediate crystalline growth front.[36] From the above observations, we conclude that larger silica spheres crystallize on a layer of smaller ones just as they do on a flat surface. This is easily understood, especially for spheres with significant differences in their diameters, since the curvature of the big spheres is larger than that of the interstitial spaces formed by the close-packing of smaller spheres.

For the spheres with similar sizes, we observed some unusual packing at the interface between the layers, reminiscent of packing seen with template-directed colloidal crystallization.[34] In our case, however, the (111) plane instead of (110) plane acts as the template for crystallization. For the case of small spheres stacked on bigger ones, the crystallization process is complex since the curvature of the interstitial spaces formed by the hexagonal close-packing of big spheres is larger than the diameter of the smaller spheres. For this reason, the smaller spheres can be trapped in the interstitial spaces at the interface between layers. Obtaining clear views of these interfaces without disrupting their structure is difficult, however. We solve this problem using macroporous polymers formed from the multilayer samples. These are faithful replicas of the starting silica multilayer colloidal crystals, and are much easier to cleave in order to image the interfaces, as shown in Figure 4.

Figure 4A shows a two-layer macroporous polystyrene multilayer, composed of a crystalline array of spherical voids of 253 nm diameter, on top of a crystalline array of 430 nm voids; Figure 4B shows a three-layer macroporous polymer (338 nm/430 nm/253 nm). The inset in Figure 4A shows a high-magnification SEM image which reveals the interface between the array of 253 nm voids and the array of 430 nm voids. The flat, close-packed arrangement of the smaller voids is clearly seen. Since the voids are an exact replication of the silica colloids used as a template in the formation of this macroporous polymer sample, the ordering of the air voids represents that of the original silica colloids. From these images, we conclude that the smaller spheres assemble as if the underlying array of bigger spheres presented a flat surface during the crystallization process. Given the aforementioned considerations, this result is somewhat surprising. Further studies using confocal microscopy may be useful for understanding this observation.[34] However, from a practical standpoint, this result implies that particle sizes for each sub-component of the colloidal multilayer crystal can be arbitrarily selected, at least within the range of colloid diameters studied to date.

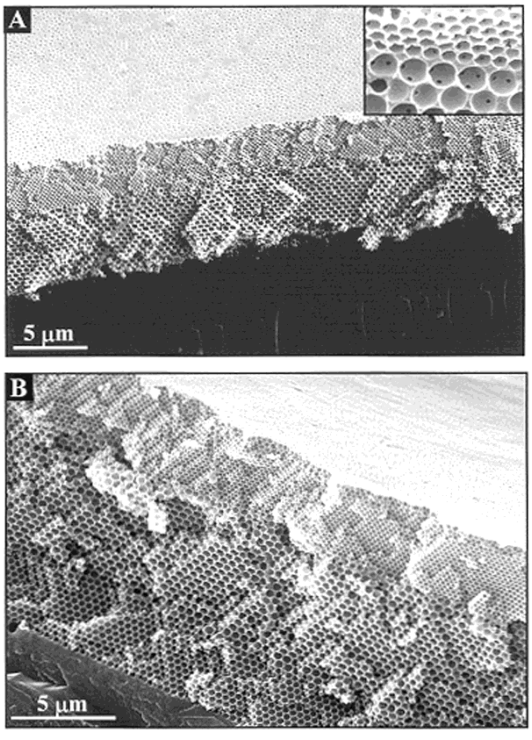

Fig. 4. Typical cross-sectional SEM images of macroporous polystyrene films made by templating from silica multilayer crystals. A) A two-layers sample composed of 253 nm voids on top of 430 nm voids. The higher magnification image in the inset shows the interfacial stacking. B) A three-layer 338 nm/430 nm/253 nm sample.

Figure 5 shows the optical transmission spectra for two three-layer silica multilayer colloidal crystals, where the three layers have been deposited in two different orderings. The

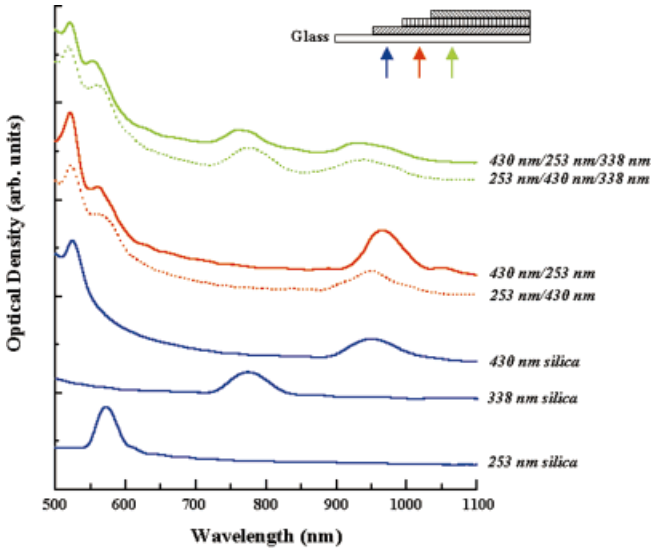

Fig. 5. Normal incidence transmission spectra of silica multilayer colloidal crystals. These curves have been vertically offset for clarity. The blue lines show the reference spectra of each individual crystal (16 monolayers of 253 nm spheres, 13 monolayers of 430 nm spheres, and 10 monolayers of 338 nm spheres). The red and green lines show the spectra from the two-layer and three-layer areas of samples with the same particle sizes but different deposition order. In both cases, the number of monolayers of each type of sphere is the same as in the individual spectra (blue curves).

blue lines represent spectra from each individual layer, while the red lines show the doubly overlapped multilayers and the green lines represent the triply overlapped multilayers. In the latter two cases, we compare doubly overlapped and triply overlapped samples with different layer orderings. The peaks around 570 nm, 764 nm and 965 nm arise from the Bragg diffraction of incident light within each layer, as seen in the blue curves. The peak positions can be related to the sphere diam-

  0935-9648/01/0603-0391 $ 17.50+.50/0

ADVANCED MATERIALS

eter and the effective refractive index of the medium using Bragg's law, $\lambda_{max} = 2n_{eff}d_{111}$, where d_{111} is the (111) lattice spacing. We have also observed an intense secondary diffraction peak from the 430 nm crystalline arrays near 520 nm. Both the large amplitude and the position of this peak are consistent with the results from previous studies of crystalline colloidal arrays.[44] We note that the spectra of the multilayer colloidal crystals have features which correspond to peaks in each of the spectra of the crystals with only one size of colloid. This correspondence confirms the high crystalline quality of each multilayer of the composite sample, and also suggests that the optical properties of the composite multilayers can be approximated from the spectra of the individual layers by a simple superposition. The similarity of the spectra for the doubly and triply overlapped regions with different layer ordering (red and green lines in Fig. 5) provides additional evidence that the interfaces do not play a significant role in the overall optical properties.

We also note that the overlapping of the secondary diffraction peak from the 430 nm colloidal layer with the 570 nm peak from the 253 nm colloidal layer produces a single, broader peak. This suggests one way to tailor the photonic bandgap properties of the multilayer colloidal crystal. To create a broader stop-band, crystals of spheres with similar sizes can be overlapped together, producing a composite film which inhibits light propagation over a wider range of wavelengths, and presumably a wider range of angles as well. To explore this idea further, we have produced a sample consisting of three layers of crystals composed of spheres of similar sizes. Figure 6A shows the transmission spectrum of a 303 nm/325 nm/338 nm sample. The green, black, and red lines represent reference transmission spectra from each individual crystal. For these non-overlapped samples, the thickness of each of the crystals is the same as that in the composite multilayer sample. We observe significant broadening of the relative width ($\Delta\lambda/\lambda$) of the stop-band in the (111) direction, from ~6–7 % for the single crystals to ~10 % for the multilayer sample. Figure 6B shows the relative insensitivity of this broader stop-band to the angle of incidence of the radiation. This result suggests that by overlapping many colloidal crystals with similar sphere sizes the effective band width can be increased; this may be a viable strategy for creating lightweight and large area optical filters.

In order to see if the optical spectrum of a multilayer colloidal crystal is determined simply by superposition of the spectra of its component crystals, we show the sum of the spectra of the individual layers in Figure 6A (dashed curve), for comparison with the measured spectrum of the multilayer film. Interestingly, the spectrum of the tri-layer crystal is similar to, but not identical to, the sum of the spectra of the three individual layers. New and fairly narrow spectral features are formed, presumably as a result of coherent interference effects between the stop-bands of the three sub-units. These features are reminiscent of "minibands", similar to the effects seen in electronic superlattices, and their presence suggests the possibility of tailoring mid-gap resonances in photonic crystals.

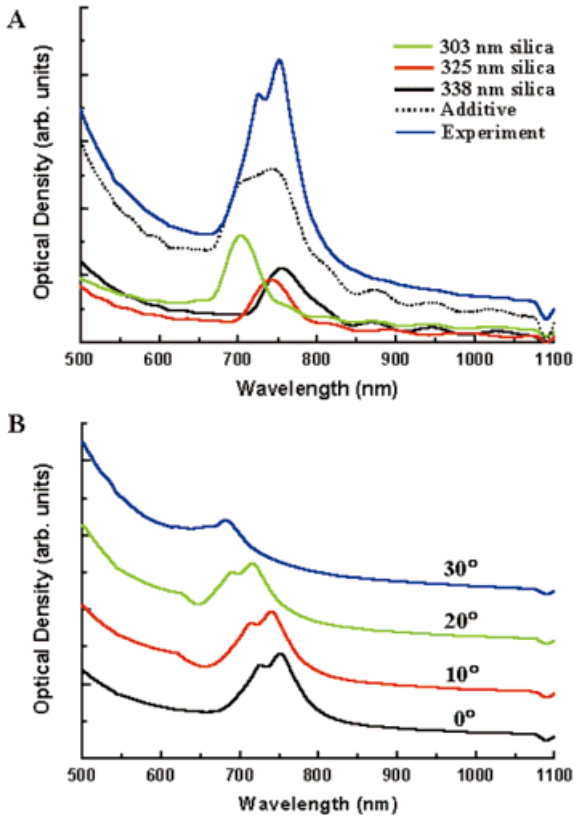

Fig. 6. A) Normal incidence transmission spectra of a 338 nm/325 nm/303 nm silica multilayer crystal (blue line). The black, red, and green lines show the reference spectra from silica crystals of 338 nm (15 monolayers), 325 nm (18 monolayers), and 303 nm (15 monolayers), respectively, each with the same thickness as the corresponding sub-unit of the multilayer sample. The dotted black line shows the sum of these three reference spectra, which may be compared with the spectrum of the multilayer sample. B) Optical transmission spectra reveal the angle dependence of the position and width of the stop-band for the 338 nm/325 nm/303 nm multilayer sample.

In summary, we have demonstrated an efficient method to fabricate colloidal crystals with multilayer structures from a variety of colloids with different sizes. These materials exhibit approximately additive photonic bandgap properties, which can be tailored by manipulating secondary diffraction, film composition, and sphere size. Although only silica multilayer colloidal crystals have been shown here, we found this method can be easily extended to other monodisperse colloids, such as polystyrene beads. By alternating deposition of silica and polystyrene layers, a one-dimensional photonic crystal with three-dimensional sub-structure could be made. Such a geometry is similar to Rugate filters and may find important application in interference coating.[45] Other non-optical applications can also be envisioned, such as the use of size-gradient macroporous polymers in membrane separations.[46] Finally, it should be possible to form a multilayer consisting of many alternating layers of two different sphere sizes. In this geometry, it would be possible to form true "superlattice" photonic crystals with strong interactions between waves diffracted over large distances. The optical properties of such systems would present an entirely different way of tailoring the photonic properties of these colloidal crystal films.

  0935-9648/01/0603-0392 $ 17.50+.50/0

Experimental

Monodisperse silica colloids with diameters ranging from 200–500 nm are synthesized following the Stober–Fink–Bohn method [47]. The as-synthesized silica sols are purified and redispersed in 200 proof ethanol by at least six centrifugation/redispersion cycles. The methods described in our previous paper [36] are used to fabricate three-dimensionally ordered planar colloidal crystals with thickness ranging from one monolayer to 50 monolayers. In short, a glass slide is immersed vertically into ~15 mL purified silica sol (1 % particle volume fraction) contained in a glass scintillation vial. After ethanol slowly evaporates, an iridescent film is formed on top of the glass slide. A large area (1 cm × 3 cm) sample can be made over 3–5 days. After each single coating is deposited, the film is taken out of the silica sol and air-dried for 10 min and then dipped again into another purified silica sol with differing particle size. This coating–drying–coating cycle can be repeated many times and each time the particle size can be arbitrary selected. The thickness of each crystalline sub-unit can be easily tuned by changing the concentration of the silica sol [36]. In this way, a layered structure with an arbitrary pattern of sphere sizes can be assembled. Macroporous polystyrene films are made by templating the colloidal crystal as described before [18].

SEM is carried out on a Philips XL30 ESEM. A CrC-100 sputtering system has been used to coat a thin layer of gold on the samples before SEM analysis. To reveal an edge appropriate for cross-sectional SEM analysis, the samples are scraped using a sharp razor blade and tilted 30–40°. Transmission spectra are obtained by using an Ocean Optics ST2000 fiber optic UV–near-IR spectrometer. An Oriel model 6000 UV lamp with 68806 basic power supply is used to polymerize styrene.

Received: October 5, 2000

[1] P. Pieranski, *Contemp. Phys.* **1983**, *24*, 25.
[2] A. P. Gast, W. B. Russel, *Phys. Today* **1998**, *51*, 24.
[3] Y. Xia, B. Gates, Y. Yin, Y. Lu, *Adv. Mater.* **2000**, *12*, 693.
[4] W. L. Vos, R. Sprik, A. van Blaaderen, A. Imhof, A. Lagendijk, G. H. Wegdam, *Phys. Rev. B* **1996**, *53*, 16 231.
[5] I. I. Tahran, G. W. Watson, *Phys. Rev. Lett.* **1996**, *76*, 315.
[6] J. D. Joannopoulos, R. D. Meade, J. N. Winn, *Photonic Crystals*: *Molding the Flow of Light*, Princeton University Press, Princeton **1995**.
[7] P. L. Flaugh, S. E. O'Donnell, S. A. Asher, *Appl. Spectrosc.* **1984**, *38*, 847.
[8] E. A. Kamenetzky, L. G. Mangliocco, H. P. Panzer, *Science* **1994**, *263*, 207.
[9] G. Pan, R. Kesavamoorthy, S. A. Asher, *Phys. Rev. Lett.* **1997**, *78*, 3860.
[10] S. Sun, B. Murray, D. Weller, L. Folks, A. Moser, *Science* **2000**, *287*, 1989.
[11] J. H. Holtz, S. A. Asher, *Nature* **1997**, *389*, 829.
[12] O. D. Velev, E. W. Kaler, *Langmuir* **1999**, *15*, 3693.
[13] O. D. Velev, T. A. Jede, R. F. Lobo, A. M. Lenhoff, *Nature* **1997**, *389*, 447.
[14] B. T. Holland, C. F. Blanford, A. Stein, *Science* **1998**, *281*, 538.
[15] G. Subramanian, V. N. Manoharan, J. D. Thorne, *Adv. Mater.* **1999**, *11*, 1261.
[16] S. H. Park, Y. Xia, *Adv. Mater.* **1998**, *10*, 1045.
[17] S. A. Johnson, P. J. Ollivier, T. E. Mallouk, *Science* **1999**, *283*, 963.
[18] P. Jiang, K. S. Hwang, D. M. Mittlman, J. F. Bertone, V. L. Colvin, *J. Am. Chem. Soc.* **1999**, *121*, 11 630.
[19] Y. A. Vlasov, N. Yao, D. J. Norris, *Adv. Mater.* **1999**, *11*, 165.
[20] P. V. Braun, P. Wiltzius, *Nature* **1999**, *402*, 603.
[21] P. Jiang, J. Cizeron, J. F. Bertone, V. L. Colvin, *J. Am. Chem. Soc.* **1999**, *121*, 7957.
[22] O. D. Velev, P. M. Tessier, A. M. Lenhoff, E. W. Kaler, *Nature* **1999**, *401*, 548.
[23] B. J. Ackerson, K. Schatzel, *Phys. Rev. E* **1995**, *52*, 6448.
[24] P. N. Pusey, W. van Megen, *Nature* **1986**, *320*, 340.
[25] J. L. Harland, S. M. Henderson, S. M. Underwood, W. van Megen, *Phys. Rev. Lett.* **1995**, *75*, 3572.
[26] C. Murray, *MRS Bull.* **1998**, *23*, 33.
[27] N. A. Clark, A. J. Hurd, B. J. Ackerson, *Nature* **1979**, *281*, 57.
[28] H. B. Sunkara, J. M. Jethmalani, W. T. Ford, *Chem. Mater.* **1994**, *6*, 362.
[29] M. Weissman, H. B. Sunkara, A. S. Tse, S. A. Asher, *Science* **1996**, *274*, 959.
[30] Z. Cheng, W. B. Russel, P. M. Chalkin, *Nature* **1999**, *401*, 893.
[31] H. Miguez, F. Meseguer, C. Lopez, A. Blanco, J. S. Moya, J. Requena, A. Mifsud, V. Fornes, *Adv. Mater.* **1997**, *10*, 480.
[32] M. Trau, D. A. Saville, I. A. Aksay, *Science* **1996**, *272*, 706.
[33] R. C. Hayward, D. A. Saville, I. A. Aksay, *Nature* **2000**, *404*, 56.
[34] A. van Blaaderen, R. Rue, P. Wiltzius, *Nature* **1997**, *385*, 321.
[35] S. H. Park, D. Qin, Y. Xia, *Adv. Mater.* **1998**, *10*, 1028.
[36] P. Jiang, J. F. Bertone, K. S. Hwang, V. L. Colvin, *Chem. Mater.* **1999**, *11*, 2132.
[37] A. S. Dimitrov, C. D. Dushkin, H. Yoshimura, K. Nagayama, *Langmuir* **1994**, *10*, 432.
[38] N. Hunt, R. Jardine, P. Bartlett, *Phys. Rev. E* **2000**, *62*, 900.
[39] C. J. Kiely, M. Brust, D. Bethell, D. J. Schiffrin, *Nature* **1998**, *396*, 444.
[40] J. V. Sanders, *Philos. Mag. A* **1980**, *42*, 721.
[41] L. V. Woodcock, *Nature* **1997**, *385*, 141.
[42] A. S. Dimitrov, K. Nagayama, *Langmuir* **1996**, *12*, 1303.
[43] J. F. Bertone, P. Jiang, K. S. Hwang, D. M. Mittleman, V. L. Colvin, *Phys. Rev. Lett.* **1999**, *83*, 300.
[44] L. Liu, P. Li, S. A. Asher, *J. Am. Chem. Soc.* **1997**, *119*, 2729.
[45] W. H. Southwell, *Appl. Opt.* **1997**, *36*, 314.
[46] R. R. Bhave, *Inorganic Membranes*: *Synthesis*, *Characteristics and Applications*, Van Nostrand Reinhold, New York **1991**.
[47] W. Stober, A. Fink, E. Bohn, *J. Colloid Interface Sci.* **1968**, *26*, 62.

Synthesis and Photonic Bandgap Characterization of Polymer Inverse Opals**

By *Hernán Míguez*, *Francisco Meseguer*, *Cefe López*,* *Fernando López-Tejeira*, and *José Sánchez-Dehesa*

Systems with spatial periodic modulation of the dielectric constant have attracted much attention from both theorists and experimentalists during the last decade.[1] These structures, known as photonic bandgap materials, would present interesting technological applications in photonics and electronics.[2] Such applications rely on the fabrication of materials with photonic crystal properties in the visible and near infrared. Colloidal systems in general, and opals in particular, have been shown to present photonic crystal properties[3,4] and other advantages in that direction. These systems can be easily fabricated and their work region tuned through the sphere diameter, covering an ample range around the visible and near infrared.[5] However, opals are most appreciated not for their own photonic properties but for their use as hosts to other materials and, especially, as matrices for the molding of inverse opals. Silica opals particularly are very useful in applications where the synthesis of the guest materials require extreme conditions, since silica is thermally stable at relatively elevated temperatures and chemically inert in the presence of most solvents (particularly organic ones).

From a practical point of view the polymer infiltration in opals, whether silica or otherwise, is relatively easy and efficient. Host matrices are also easily removed by means of either a chemical attack or an optically induced degradation;

[*] Dr. C. López, H. Míguez, Dr. F. Meseguer
Instituto de Ciencia de Materiales de Madrid (CSIC)
Cantoblanco, E-28049 Madrid (Spain)
E-mail: cefe@icmm.csic.es
and
Centro Tecnológico de Ondas, Unidad Asociada CSIC-UPV
Edificio Nuevos Institutos II, Universidad Politécnica de Valencia
Av. Naranjos s/n, E-46022 Valencia (Spain)
Dr. F. López-Tejeira, Dr. J. Sánchez-Dehesa
Dep. Física Teórica de la Materia Condensada
Universidad Autónoma de Madrid
Cantoblanco, E-28049 Madrid (Spain)

[**] This work was partially financed by the Spanish CICyT project No. MAT97-0698-C04, European Commission project IST-1999-19009 PHOBOS project, and the Fundación Ramón Areces. We also acknowledge MIT for photonic band structure calculations.

  0935-9648/01/0603-0393 $ 17.50+.50/0